ELSEVIER

Polymer 41 (2000) 9147–9154

polymer

www.elsevier.nl/locate/polymer

Structure and properties of 3-alkoxy substituted polythiophene synthesized at low temperature

Xiao Hu*, Lingge Xu

School of Materials Engineering, Nanyang Technological University, Nanyang Avenue, Singapore 639798, Singapore

Received 5 January 2000; received in revised form 3 April 2000; accepted 11 April 2000

Abstract

In order to get a better knowledge on the influence of the introduction of alkoxy group on the thermal and optical properties of the conducting polythiophene derivatives, poly(3-alkoxythiophene)s have been chemically polymerized using iron (III) chloride as oxidizing agent under lower temperature and controlled addition of monomer. The polymers so obtained have relatively higher molecular weight, less defects and increased crystallinity as compared with those produced at room temperature. Their X-ray diffraction patterns support the stacking structure of polymer chain as proposed for poly(3-alkylthiophene). Their thermal stability and transition behavior are studied using TGA and MDSC techniques and compared with those of corresponding poly(3-alkylthiophene). The glass transition and the onset of decomposition temperature of the polymer decrease with the increase of the side chain length and the glass transition is dependent on the flexibility of the side chain introduced. The extent of conjugation of these polymers are higher than that of poly(3-alkylthiophene) and the polymers exhibit interesting fluorescence phenomena. Moreover, these polymers are photosensitive and the preliminary results of the interaction between the polymer and the light are also reported.

Keywords: Functionalized polythiophene; Poly(3-alkoxythiophene); Conjugation

1. Introduction

Functionalized polythiophenes have received considerable attention owing to their interesting electrical, electrochemical and optical properties [1–3]. The introduction of flexible pendant chains onto the backbone improves the solubility and processability allowing a more complete characterization of the materials [4,5]. Also, such introduction modifies the electronic properties of the polymer [6] enlarging the possibilities for industrial applications. For instance, based on the above method a good understanding of the fundamental molecular features necessary to achieve and control the electronic properties has been developed for poly(3-alkylthiophenes) (P3ATs). Major improvements have been achieved in the synthetic approaches, studies on the effect of the substituents as well as the polymerization methods [7–10]. Many 3-substituted polythiophene derivatives with thermochromic [11], solvatochromic [12] and photoluminence behaviors [13] have been produced, meanwhile the structure–property relationship has also been investigated systematically [8,9].

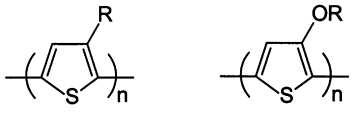

P3AT P3AOT

R = alkyl group

Polythiophenes with substituents other than alkyl groups have also been investigated, among which those with electron-donating alkoxy groups have displayed promising electrical and optical properties [14,15]. Incorporation of an alkoxy group to the 3-position of the thiophene ring yields polymers with an optical absorption maximum at 475–530 nm higher or comparable with those of P3ATs. This can be attributed to both the electron-donating effect of alkoxy group and the more coplanar conformation of poly(3-alkoxythiophene) (P3AOT) as compared to that of P3AT [14]. It was observed that unlike P3AT, poly(3-octoxythiophene) adopts a coplanar structure (long wavelength absorption) and it also appears to remain rather conjugated even at high temperatures as indicated by the temperature-dependent UV–Vis absorption spectra [16]. However, these P3AOTs only have a lower conductivity

* Corresponding author. Tel.: +65-790-4610; fax: +65-792-6559.
E-mail address: asxhu@ntu.edu.sg (X. Hu).

0032-3861/00/$ - see front matter
PII: S0032-3861(00)00299-8

of about 10^{-4}–10^{-2} S/cm after electrochemical doping due to lower molecular weight and irregular structure [17–19]. The polymers are soluble in organic solvents even after doping up to 20%. As is known, the advantage of the P3AOT comes from the electron-donating effect of the alkoxy group, which decreases the oxidation potential of these polymers and consequently, stabilizes the conducting states [20]. Moreover, the alkoxy substituents that can delocalize the π-electrons often enhance fluorescence because they tend to increase the transition probability between the lowest excited singlet state and the ground state [21]. In this way the alkoxy substituents play an important role in the properties of P3AOTs. In addition, the introduction of alkoxy functional group may increase the hydrophilicity of the polymer, which enables P3AOT to form a stable Langmuir–Blodgett film on pure water subphase. So far, to our knowledge, unlike P3ATs, study on the structure–property relationship of P3AOTs has not been performed systematically. Therefore, in this paper we describe the synthesis and comprehensive characterization of these polymers in order to get a better knowledge of the influence of the introduction of alkoxy group on the thermal and optical properties of these conducting polythiophene derivatives.

2. Experimental

2.1. Synthesis of monomers

3-Methoxythiophene was prepared by following a procedure for the Cu(I)-catalyzed methoxylation of 3-bromothiophene [22]. Other 3-alkoxythiophenes (butoxy, hexoxy and octoxy) were prepared by condensation of 3-methoxythiophene with 1-alkanol in the presence of 1–10 mol% (protonic) acid catalyst $NaHSO_4$ under reflux for 3–5 h. The pure monomers were obtained after distillation under reduced pressure [23].

2.2. Polymerization

$FeCl_3$ (2.6 g, 16 mmol) was quickly weighed in a reaction vessel and kept under nitrogen. Anhydrous $CHCl_3$ (15 ml) was added into the vessel at 0–2°C followed by monomer (4 mmol) in $CHCl_3$ (5 ml) dropwise over a period of 30 min. Then the mixture was stirred for 2 h. The polymer was washed with methanol, dedoped by stirring in 50% aqueous hydrazine monohydrate and washed with water and methanol, then dried under dynamic vacuum (0.3–0.4 mbar). The neutral polymers, poly(3-methoxythiophene), poly(3-butoxythiophene), poly(3-hexoxythiophene) and poly(3-octoxythiophene) were designated as P3MOT, P3BOT, P3HOT and P3OOT, respectively.

2.3. Characterization

Gel permeation chromatographic (GPC) analyses were carried out for the measurement of molecular weight using a Waters 600E system controller and Waters 410 differential refractometer together with Phenogel 5 linear (2) column calibrated using polystyrene standards and THF as eluent. FT-IR spectra of monomers and polymers dispersed in KBr disks were recorded on a Perkin–Elmer System 2000 FT-IR Spectrometer for the structural analysis. The ^1H NMR spectra were performed on a Bruker AC-300 (300 MHz) plus Fourier Transform Instrument using tetramethylsilane and $CDCl_3$ as an internal reference, respectively. X-ray diffractions of polymer films on glass slides were measured using a Rigaku Rint 2000 X-ray Diffractometer. Thermogravimetric analysis (TGA) of polymer powders were conducted on a TA Instruments Thermal Analyst 2100 system with a Hi-Res TGA 2950 thermogravimetric analyzer. A heating rate of 10°C/min with an air flow of 60 ml/min was used, the runs being conducted from 25 to 800°C. Modulated DSC (MDSC) measurement was carried out on a TA Instruments DSC 2920 Modulated DSC. Thermograms of the heating run were recorded at a heating rate of 5°C/min, a modulation period of 60 s and a modulation amplitude of ^ 1°C from −50 to 150°C under nitrogen purge. UV–Vis spectra were recorded from dilute solutions or thin films on an indium–tin oxide (ITO) glass plate on a Shimadzu UV-2501PC UV–Vis Recording Spectrophotometer. Fluorescence measurements were conducted on a Shimadzu RF5000 Spectrofluorophotometer equipped with a xenon lamp (150 W) as the source. Irradiation of the polymer solution was carried out in the sample compartment of this spectrofluorophotometer with the slit width set at 5 nm and the source set at desired wavelength. The samples were irradiated for different time intervals and subsequently both the fluorescence and the UV–Vis spectra were recorded.

3. Results and discussion

3.1. Solubility and molecular weight

All these four polymers were dark red-violet powders after washing with methanol and subsequent reduction by chemical means using an aqueous solution of hydrazine. Elemental analysis reveals that the Fe contents (wt%) in the dedoped samples were 1.54, 1.27, 1.06 and 0.85% for P3MOT, P3BOT, P3HOT and P3OOT, respectively, indicating a rather low doping level in these dedoped polymers. P3BOT, P3HOT and P3OOT were found to be soluble in chloroform, THF and methylene chloride but P3MOT was only partially soluble in these solvents. Uniform films of P3BOT, P3HOT and P3OOT can be easily formed from chloroform solutions. However, the film of P3MOT on glass or ITO-glass substrate is not continuous and with many cracks. The polymers are stable if they are stored in dark. This can be corroborated by the UV–Vis spectra of the polymers. No distinguishable change was observed in the UV–Vis region between the freshly-made samples and those stored in dark for two months. The polymerization

Table 1
Average molecular weights of P3AOTs relative to polystyrene standards (M_n, number-averaged molecular weight; PDI, polydisposity index; DP, degree of polymerization)

Polymer	M_n	PDI	DP
P3MOT	1875	1.25	17
P3BOT	2050	1.26	13
P3HOT	2270	1.26	13
P3OOT	2780	1.13	13

condition in some of the previous works reported by other groups [24,25] was at room temperature and the reaction time was 24 h. However, we found that the polymerization carried out under low temperature 0°C and the dropwise addition of monomer over a period of 30 min could yield a polymer with relatively higher molecular weight although the reaction time was only 2 h. This was indicated by the GPC results of the corresponding polymers, which are listed in Table 1. The degree of polymerization (DP) of the polymer is higher than that previously reported for poly(3-heptoxythiophene) generated at room temperature for 24 h, which is only 7 [24] and is comparable to that of P3MOT prepared by dehalogenation polycondensation using zero-valent nickel complexes [26]. However, it is lower than those of P3ATs [8].

3.2. FT-IR and NMR spectroscopy

Fig. 1 depicts the FT-IR spectra of the four polymers, the presence of the alkoxy pendants is evidenced from C–H stretching at ca. 2850 and 2950 cm^{-1}due to $-CH_2-$ and $-CH_3$ groups. Ring vibrational modes are seen at 1525, 1450 and 1350 cm^{-1}. The band at 1060 cm^{-1} is assigned to C(ring)–O–C stretching. The vibrational band at 810 cm^{-1} is attributable to $C-H_\beta$ out-of-plane deformation mode of thiophene rings [27]. The absorption peak at 720 cm^{-1} ascribable to $C-H_\alpha$ out-of-plane deformation of thiophene rings is found to be rather weak. The $C-H_\beta$ deformation band is weak in comparison with that of P3AT [9] indicating that some β-defects exist in the polymer, which is attributed to the strong electron-donating nature of the alkoxy pendant making the β-position more reactive in 3-alkoxythiophene than in 3-alkylthiophene. However, the intensity ratio of $C-H_\beta$ to $C-H_\alpha$ deformation bands is almost the same as that of P3AOTs prepared by dehalogenation polycondensation using zero-valent nickel complexes [26], which is believed to have a well-defined linkage between the monomeric units. Therefore, $\alpha-\alpha'$ coupling can be considered predominant during the polymerization process carried out at 0°C. The presence of two bands at ca. 2850 and 2950 cm^{-1} suggests that the alkoxy chain remains intact after polymerization. The relative intensity of these two bands to the band at 1060 cm^{-1} was found to increase with an increasing length of the alkoxy pendant chain.

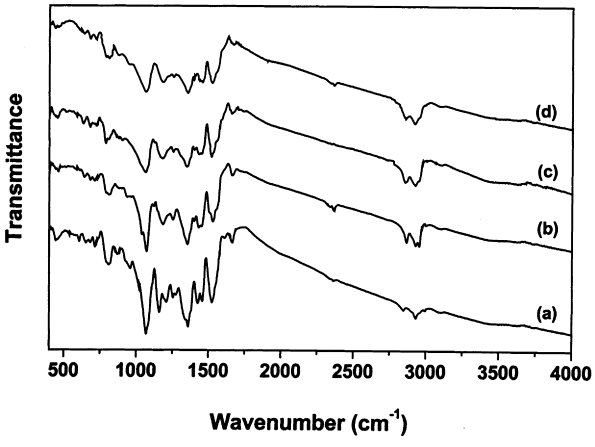

Fig. 1. FT-IR spectra of P3AOTs: (a) P3MOT; (b) P3BOT; (c) P3HOT; and (d) P3OOT.

In addition, the ^1H NMR spectra of the polymers corroborate the $\alpha-\alpha'$ linkage of the adjacent thienyl rings. Typically for P3HOT, no peaks assigned to 2- (δ ca. 6.15 ppm) and 5-position (δ ca. 6.80 ppm) hydrogen atoms are observed in these low-temperature polymerized sample as opposed to those synthesized at room temperature [25]. However, in the aromatic region two major peaks at 6.84 (HT–HT) and 6.97 ppm (TT–HT) and two poor-resolved weak peaks at 6.90 (HT–HH) and 7.04 ppm (TT–HH) corresponding to four triad regioisomers in the 3-substituted polythiophene main-chain [10] are evident implying a regiorandom structure. The peak at 4.10 ppm and a small shoulder at 3.90 ppm are observed for the α-methylene protons of the alkoxy group, which can be attributed to a mixture of head-to-tail and head-to-head linkages along the polymer mainchain. Similar observations were obtained for all other P3AOTs (see Fig. 2).

3.3. X-ray diffraction

X-ray diffraction patterns of the polymer films on glass slide cast from chloroform solution are shown in Fig. 3 and their characteristic angles at intensity maxima and corresponding value of *d*-spacings calculated are listed in Table 2.

Except for P3MOT, which only depicts a broad amorphous peak with a maximum intensity at 22.8°, each of the other three polymers has one diffraction peak at low angle region corresponding to first-order reflection in addition to a broad amorphous peak at wide angle region, respectively. The crystallinity of P3AOT is lower than that of P3AT [8] as indicated by the less sharp diffraction peak in the XRD spectrum. Unlike the case of P3ATs, in which three orders of reflection were present, only the first-order reflection of P3AOT was observed. This indicates that a higher degree of space filling of the alkyl side chain exists in P3ATs than in P3AOTs [8] probably due to less β-defects in P3ATs than in P3AOTs and also the presence of more polar alkoxy groups which hinders the intercalation of the

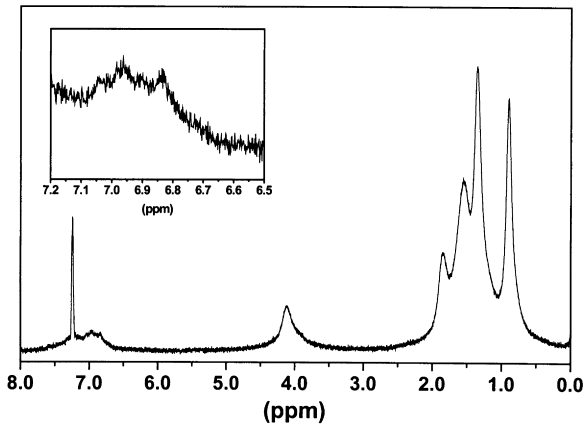

Fig. 2. ^{1}H NMR spectrum of P3HOT. The inset is the expanded aromatic region.

side chains. The corresponding *d* spacing is found to increase with an increasing side chain length, which is consistent with the case of P3ATs. This also supports the previously proposed structure for the packing of main chain and side chain in P3ATs [8]. Similarly, the stacks of planar thiophene main chain in P3AOTs are spaced by the alkoxy side chain. Apparently, the *d* spacing of each P3AOT is larger than that of the corresponding P3AT with the same carbon atoms in the side chain due to the incorporation of one more oxygen atom. When comparing the *d* spacing in the low angle region for these two series of polymers, it is found that with every increase of two methylene groups, the *d* spacing increases ca. 3–4 Å. This means that with one methylene group incorporated in, the *d* spacing increases by only ca. 1.5–2 Å. However, with the incorporation of one oxygen atom, the *d* spacing increases by ca. 3–4 Å. Actually, the C–C bond length (~1.5 Å) is longer than C–O bond length (~1.4 Å). This observation also suggests that not much intercalation exist in P3AOTs because of repulsion due to the presence of oxygen. Another diffraction centered at ca. 22° corresponds to a spacing of ca. 4.0 Å. This side-chain-length-independent spacing can be attributed to the spacing between two successive stacking planes of coplanar subchains as has already been assigned for P3ATs [8]. On examination of the peak shape at low angle, it is found that with increase of the alkoxy side-chain length, the diffraction peak becomes sharper and sharper indicating an increase in crystallinity. Meanwhile, since it is agreed that the amorphous structure can be attributed to a cross-linking by α–β' coupling between thiophene rings, the P3AOTs synthesized by our method are expected to have less β-defects in comparison with those produced at room temperature, whose diffraction pattern shows a totally amorphous phase [24].

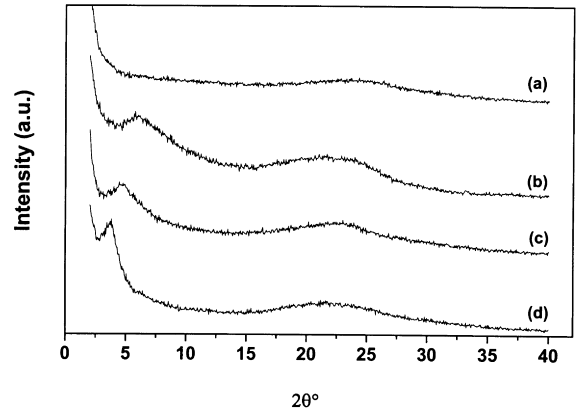

Fig. 3. X-ray diffraction patterns of P3AOT films cast from chloroform solutions: (a) P3MOT; (b) P3BOT; (c) P3HOT; and (d) P3OOT.

Table 2
X-ray diffraction 2θ positions and calculated *d* spacing of P3AOTs and P3ATs (results of poly(3-alkylthiophenes) were taken from Ref. [8]): methyl (P3MT); butyl (P3BT); hexyl (P3HT); and octyl (P3OT)

Polymer	$2\theta^\circ$ (*d* spacing, Å)	
	Low angle	Wide angle
P3MOT/P3MT	– (–)/14.0 (6.0)	22.8 (4.0)/24.6 (3.6)
P3BOT/P3BT	5.8 (15.5)/7.1 (12.4)	21.4 (4.1)/23.3 (3.8)
P3HOT/P3HT	4.5 (19.8)/5.3 (16.8)	22.3 (4.0)/23.4 (3.8)
P3OOT/P3OT	3.7 (23.9)/4.6 (19.4)	21.8 (4.1)/23.6 (3.8)

3.4. Thermal analysis (TGA and MDSC)

TGA curves of P3AOTs are shown in Fig. 4. The polymers depict two major though not completely distinct weight-loss steps in the temperature range of 25–800°C in air. The first step is ascribable mainly to the loss of the alkoxy side chain [27] and the amount of this weight loss is found to increase with pendant chain length as can be seen from Table 3. The onset temperature of 3% weight loss for the polymer is found to decrease with the increasing side-chain length. This decreasing thermal stability with the increase of side-chain length was also observed in P3ATs [28]. However, this onset temperature of weight loss is higher than those of other 3-ether-substituted polythiophenes, poly(3-heptoxy-4-methylthiophene) (133°C) and poly[3-(2-butoxyethoxy)-4-methylthiophene] (164°C) [24], but is much lower than those of P3ATs, which is in the range of 280–310°C. This is attributed to the presence of alkoxy pendant groups which makes the system more reactive and easily to be oxidized. The second weight loss step, which took place in the temperature range of ca. 400–800°C corresponds to the degradation of polymer backbone leaving behind a residue content of less than 7%. On close examination on the weight loss and derivative weight curves, it is found that the complete decomposition temperature of polymer increases with the increasing pendant chain length, probably ascribable to the occurrence of cross-linking in polymer with longer side chain during the TGA scan [29].

Modulated DSC (MDSC) has the capability to detect the multiple transitions involving endothermic and exothermic processes [30]. Therefore, it was employed to study the

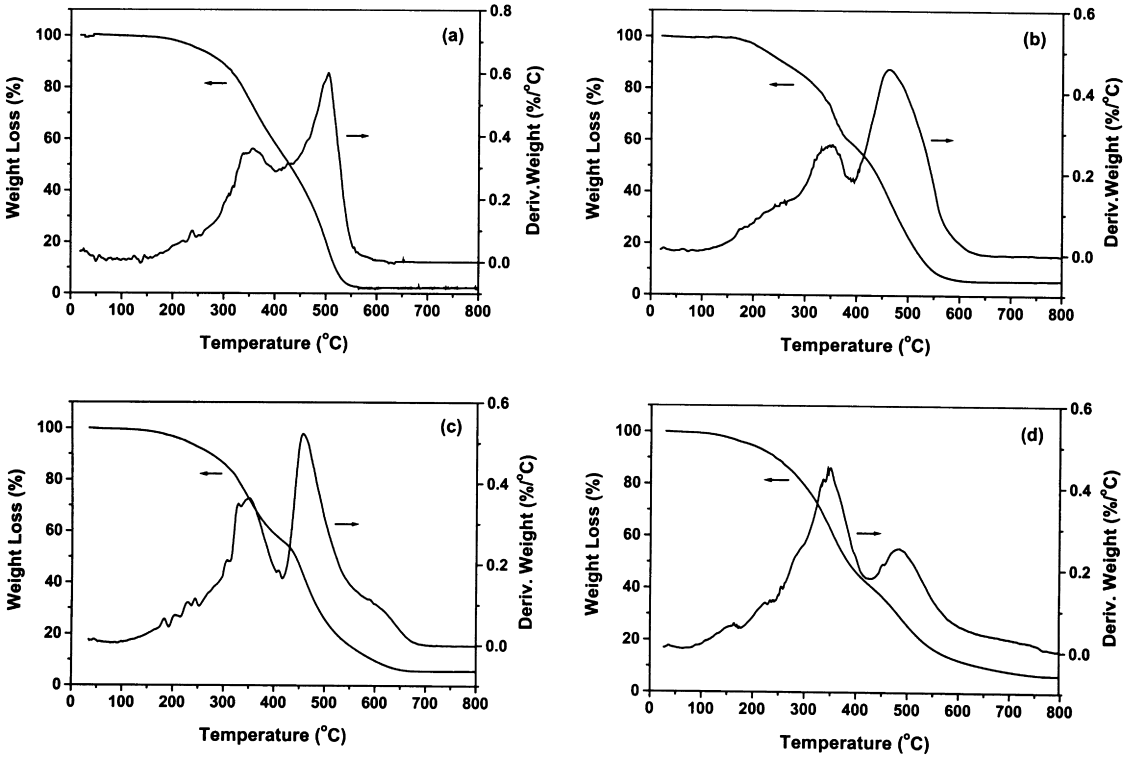

Fig. 4. TG–DTG curves of P3AOTs: (a) P3MOT; (b) P3BOT; (c) P3HOT; and (d) P3OOT.

thermal transition properties of P3AOTs. When the samples were subjected to the first run from −50 to 150°C, the thermal transition process was not clearly detected. However, after natural cooling to room temperature, the second run displayed an apparent transition step as indicated by the reversing heat flow curves, which corresponds to the glass transition. The temperatures of this transition determined (T_g) are listed in Table 3.

Similar to that of P3AT, the T_g of P3AOT decreases with increasing side-chain length attributable to the fact that the longer pendant chains provide a higher free volume, allowing the molecular chains to move or realign more easily and therefore reducing the glass transition temperature. When comparing the T_gs of P3AOTs and those of P3ATs, it is found that the T_gs of P3BOT, P3HOT and P3OOT are slightly higher than the corresponding P3BT, P3HT and P3OT, respectively. This can be explained by the effect of the less flexible alkoxy side chains in P3AOT as compared with the more flexible alkyl pendants in P3AT, since more flexible side chain may lead to the decrease of T_g.

For P3HOT and P3OOT, in addition to the presence of T_g, a small melting peak was observed in the thermogram. The melting temperatures are shown in Table 3. The lower melting temperature of them as compared with corresponding P3ATs is probably related to the lower molecular weight and lower crystallinity of P3AOTs. Similar to P3MT and P3BT, no evident melting peak was observed for P3MOT and P3BOT in the temperature range of −50–150°C.

Table 3
TGA results and transition temperature of P3AOTs (T_{os}: onset temperature of weight loss at 3%; T_{cd}: completely decomposed temperature; T_g: glass transition temperature; T_m: melting point of polymer)

Polymer	T_{os} (°C)	Weight loss (%)		Residue (%)	T_{cd} (°C)	T_g (°C)	T_m (°C)
		1st Step	2nd Step				
P3MOT	220	39.7 (27.7)[a]	54.9	2.4	600	66.2	–
P3BOT	200	40.0 (47.4)[a]	51.4	5.6	650	58.0 (50.2)[b]	–
P3HOT	194	43.3 (55.5)[a]	48.0	5.7	700	20.2 (10.0)[c]	93.7 (170)[d]
P3OOT	163	59.2 (61.4)[a]	36.0	6.7	800	−12.8 (−14.2)[b]	86.2 (127)[d]

[a] Weight fraction of pendant alkoxy group.
[b] T_g of P3ATs determined by DSC from Ref. [8].
[c] T_g of P3HT determined by MDSC in our lab.
[d] T_m of P3ATs determined by MDSC in our lab.

Table 4
UV–Vis absorption and emission bands of P3AOTs (ϵ_{max}: extinction coefficient at absorption maximum in $CHCl_3$ and the concentration is based on monomeric unit)

Polymer	Absorption max. (nm)		Emission (nm)		ϵ_{max} (10^3 M^{-1} cm^{-1})
	In $CHCl_3$	Film	Before irradiation	After irradiation (40 min)	
P3MOT	465	483	556	536 (523)[a]	2.6
P3BOT	495	520	556	541	3.4
P3HOT	520	550	582	550	6.4
P3OOT	505	524	572	541	3.7
P3HT	435	–	570	–	8.8

[a] Values in parentheses correspond to the shoulder peak.

3.5. UV–Vis and fluorescence spectroscopy

The UV–Vis spectra of P3AOTs in chloroform solution and film were measured and the maximum absorption bands are listed in Table 4. Typical spectra of P3HOT are shown in Fig. 5. P3HOT exhibits a maximum absorption band at 520 nm in chloroform solution and at 550 nm in the film. This indicates that the packing of polymer chains in the condensed phase is anticipated to favor a coplanar arrangement of the adjacent thiophene rings, which results in a bathochromic shift in the absorption maximum in comparison with the solution-phase polymer. In going from P3MOT to P3HOT, this band also exhibits a bathochromic shift (decrease in $\pi-\pi^*$ transition energy) ascribable to so-called "zipper effect", a side-by-side overlap of the neighboring methylene segments, which increases the coplanarity of the polymer backbone resulting in longer effective conjugation length [31]. However, with further increase of the side chain length as in P3OOT, the absorption band slightly shifts to shorter wavelength in comparison with P3HOT. This could be attributable to the increased steric hindrance when the side chain is too long and this effect is predominant in this case leading to a decrease in the conjugation length. When compared with those of P3ATs, it is found that these P3AOTs have higher conjugation length than the corresponding regiorandom P3ATs and higher than or comparable to those regioregular P3ATs [7,10]. This can be attributed to the electron-donating properties of the alkoxy groups as well as a more coplanar conformation in these P3AOTs as compared to P3ATs [14]. However, the maximum extinction coefficient of P3AOT [32], ϵ_{max}, is slightly lower than that of P3HT [33], probably due to the difference in solvent–polymer interaction and difference in the response to the oxygen existing in the solvent between P3AOT and P3AT [34].

In order to study the optical properties of these polymers, the fluorescence measurements of dilute polymer solutions were performed on a spectrofluorophotometer equipped with a 150 W Xenon lamp. Interestingly, we found the spectrum changed with the prolonged time of irradiation by the light source set at desired wavelength (the maximum absorption wavelength of the corresponding polymer solution in chloroform). Typically, as shown in Fig. 6, the emission of P3OOT was at 572 nm in the first scan when excited at 505 nm. With increasing the irradiation time to ca. 10 min, the emission exhibited a blue shift to 557 nm meanwhile its intensity decreased. However, with further increase of the irradiation time to ca. 40 min, the emission shifted further to 541 nm with its intensity increased. The reaction in this process is believed to involve photobleaching via a photochemical 1,4-Diels–Alder addition of

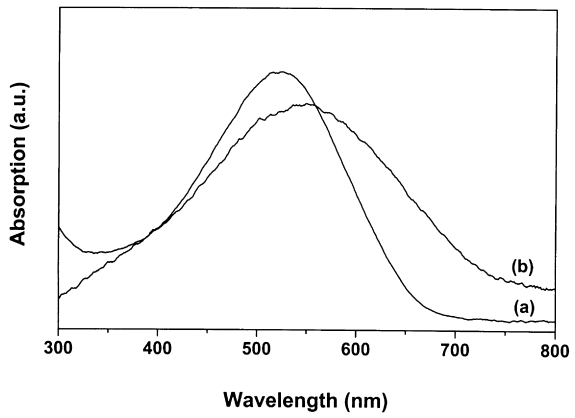

Fig. 5. UV–Vis spectra of P3HOT: (a) in chloroform solution; and (b) film.

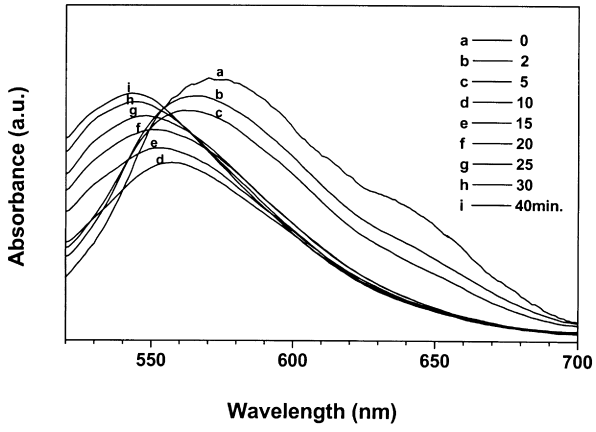

Fig. 6. Fluorescence spectra of 10^{-5} M P3OOT in chloroform solution after irradiation by 505 nm light for different periods of time.

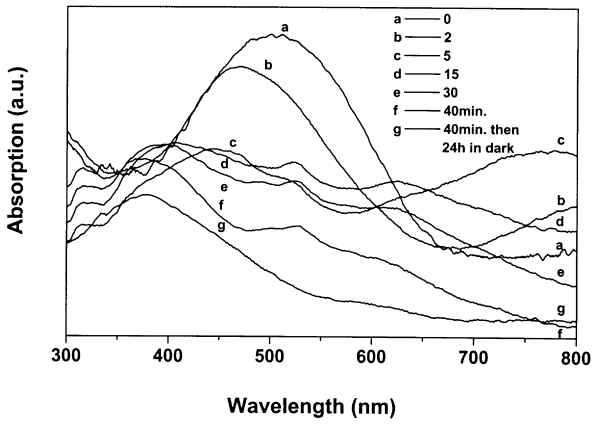

Fig. 7. UV–Vis spectra of 10^{-5} M P3OOT in chloroform solution after irradiation by 505 nm light for different periods of time.

photosensitized singlet oxygen with thienyl units, which results in the formation of products, sulfine or diketone [35,36] and a diminished state of conjugation [37]. Consequently, the absorption and emission depicted a blue-shift. This is also indicated by the corresponding UV–Vis spectra of the system after irradiation as shown in Fig. 7. The decrease in fluorescence when the system was irradiated in the beginning is most likely a result of both the disruption of conjugation and intramolecular quenching of the excited singlet state by sulfine or diketone residues similar to the case of P3ATs [34]. However, in contrast to P3ATs, as the irradiation time prolonged, the fluorescence intensity of the P3OOT system increased till a maximum was reached after about 1 h, which is anticipated to relate to the generation of other photolyzed fluorescent fragments or involve other photochemical reaction pathway. The detailed mechanism is currently under investigation.

Fig. 7 shows the UV–Vis spectra of P3OOT in chloroform solution after irradiation by 505 nm light for different periods of time. Once the system was irradiated, the π-conjugated polymer was excited and resulted in the formation of electron–hole pairs, polarons, and bipolarons rather than discrete excited singlet and triplet states [34], this is indicated by the broad polaronic band at ca. 800 nm (curves b and c). However, this band became weaker as the irradiation time prolonged while the other two bands at ca. 530 and 630 nm (curves d–f), which are also attributed to the excited states, became more evident. This observation is quite different from that for P3ATs [34] and these states are believed to be responsible for the increase in the fluorescence intensity as mentioned above. However, further investigation by other spectroscopic techniques, e.g. FT-IR, NMR or GPC needs to be carried out.

4. Conclusions

Chemical polymerization of 3-alkoxythiophene under lower temperature and controlled addition of monomer helps to obtain polymers with relatively higher molecular weight and less defects. With the increase in the side chain length, the polymer shows an increase in crystallinity, however, it is lower than that of poly(3-alkylthiophene). The polymers exhibit two thermal weight-loss steps corresponding to cleavage of side chain and degradation of backbone, respectively. The thermal stability of the alkoxy-substituted polythiophene is poorer than that of poly(3-alkylthiophene). The glass transition of the polymer depends on the length and flexibility of the pendant groups. The lower melting temperature of P3HOT and P3OOT as compared with corresponding P3ATs is probably related to the lower molecular weight and lower crystallinity of P3AOTs. Poly(3-alkoxythiophene) has a longer effective conjugation length than poly(3-alkylthiophene) due to both the stronger electron-donating property of the alkoxy groups and the more coplanar conformation of poly(3-alkoxythiophene). Poly(3-alkoxythiophene)s are fluorescent polymers and are photosensitive to UV–Vis light. The photochemical reaction is believed to involve photobleaching via a 1,4-Diels–Alder addition of photosensitized singlet oxygen with thienyl units as already proposed for poly(3-alkylthiophene) leading to disruption of conjugation. However, the mechanism and the increase in the fluorescence intensity after a certain period of irradiation need to be further investigated.

Acknowledgements

The authors thank the Ministry of Education of Singapore for financial aid through the Academic Research Funding ARC 9/97, and National Science and Technology Board of Singapore for additional financial support.

References

[1] Zotti G, Salmaso R, Gallazzi MC, Marin RA. Chem Mater 1997;9:791.
[2] Zotti G, Marin RA, Gallazzi MC. Chem Mater 1997;9:2945.
[3] Levesque I, Leclerc M. Chem Mater 1996;8:2843.
[4] Sato MA, Tanaka S, Kaeriyama K. J Chem Soc Chem Commun 1986:873.
[5] Yamamoto T, Komarudin D, Arai M, Lee B-L, Suganuma H, Asakawa N, Inoue Y, Kubota K, Sasaki S, Fukuda T, Matsuda H. J Am Chem Soc 1998;120:2047.
[6] Roncali J. Chem Rev 1997;97:173.
[7] McCullough RD, Lowe RD, Jayaraman M, Anderson DL. J Org Chem 1993;58:904.
[8] Chen S-A, Ni J-M. Macromolecules 1992;25:6081.
[9] Tashiro K, Minagawa Y, Kobayashi M, Morita S, Kawai T, Yoshino K. Synth Met 1993;55–57:321.
[10] Chen T-A, Wu X, Rieke RD. J Am Chem Soc 1995;117:233.
[11] Inganas O, Salanek WR, Osterholm JE, Laakso J. Synth Met 1988;22:395.
[12] Rughooputh SDDV, Hota S, Heeger AJ, Wudl F. J Polym Sci: Polym Phys Ed 1987;25:1071.
[13] Xu B, Holdcroft S. Macromolecules 1993;26:4457.
[14] Leclerc M, Daoust G. Synth Met 1991;41:529.

[15] Dietrich M, Heinze J. Synth Met 1991;41:503.
[16] Roux C, Leclerc M. Makromol Chem 1993;194:869.
[17] Feldhues M, Kampf G, Litterer H, Mecklenburg T, Wegener P. Synth Met 1989;28:C487.
[18] Blankespoor RL, Miller LL. J Chem Soc Chem Commun 1985:90.
[19] Chang AC, Blankespoor RL, Miller LL. J Electroanal Chem 1987;236:239.
[20] Tanaka S, Sato MA, Kaeriyama K. Synth Met 1988;25:277.
[21] Willard HH, Merritt Jr. LL, Dean JA, Settle FA. Instrumental methods of analysis. 6th ed.. Belmont, CA: Wadsworth, 1981 (p. 107).
[22] Keegstra MA, Peters THA, Brandsma L. Tetrahedron 1992;48: 3633.
[23] Wegener P, Feldhues M, Litterer H. Ger Offen 1989; DE 3,804,522: p. 7.
[24] Chen S-A, Tsai C-C. Macromolecules 1993;26:2234.
[25] Daoust G, Leclerc M. Macromolecules 1991;24:455.
[26] Miyazaki Y, Kanbara T, Osakada K, Yamamoto T. Chem Lett 1993:415.
[27] Themans B, Salaneck WR, Bredas JL. Synth Met 1989;28:C359.
[28] Wang Y, Rubner MF, Buckley LJ. Synth Met 1991;41:1103.
[29] Wang Y, Rubner MF. Synth Met 1990;39:153.
[30] Tomasi C, Mustarelli P, Hawkins NA, Hill V. Thermochim Acta 1996;278:9.
[31] Tashiro K, Minagawa Y, Kobayashi M, Morita S, Kawai T, Yoshino K. Synth Met 1993;55-57:321.
[32] Lakowicz JR. Principles of fluorescence spectroscopy. New York: Plenum Press, 1983 (p. 47).
[33] Linton JR, Frank CW, Rughooputh SDDV. Synth Met 1989;28:C393.
[34] Holdcroft S. Macromolecules 1991;24:4834.
[35] Skold CN, Schlessinger RH. Tetrahedron Lett 1970:791.
[36] Wasserman HH, Stehlow W. Tetrahedron Lett 1970:795.
[37] Abdou MSA, Holdcroft S. Macromolecules 1993;26:2954.